Nuclear Science and Techniques (2024) 35:137
https://doi.org/10.1007/s41365-024-01487-1

Overview of SSRF phase-II beamlines

Ren-Zhong Tai[1] · Zhen-Tang Zhao[1]

Received: 13 November 2023 / Revised: 22 January 2024 / Accepted: 8 February 2024 / Published online: 26 July 2024

Abstract
The SSRF phase-II beamline project was launched in 2016. Its major goal was to establish a systematic state-of-the-art experimental facility for third-generation synchrotron radiation to solve problems in cutting-edge science and technology. Currently, the construction is fully completed. All 16 newly built beamlines with nearly 60 experimental methods passed acceptance testing by the Chinese Academy of Sciences and are in operation.

Keywords SSRF phase-II beamline project · Accelerator upgrade · User laboratory · User data center · Beamline technique support

1 Introduction

Shanghai Synchrotron Radiation Facility (SSRF) is one of the advanced third-generation synchrotron radiation facilities in the world [1]. Since its official start of operation in May 2009, SSRF has provided user beam time of about 522,820 h and served more than 40,000 users coming from universities, institutes, hospitals, and high-tech companies from home and abroad. Over 10,000 papers have been published based on the experiments conducted at the SSRF.

However, even though a number of beamlines were built in Phase-I [2], and even with the addition of dedicated beamlines built subsequently, the SSRF still could not meet the huge user demand. In this context, the SSRF Phase-II Beamline Project proposed building 16 state-of-the-art beamlines, realizing nearly 60 new experimental methods, and equipping them with offline user experimental assistance support [3, 4]. The latest beamline layout of the SSRF is shown in Fig. 1. This new experimental ability is mainly reflected in the following aspects:

- *Energy range*: Many enhanced photon energy options such as high-brightness infrared for molecular structure analysis, tender X-rays for elemental analysis of P, S, and Cl in environmental science, ultrahard X-rays for structural analysis of aircraft engine materials, and γ-rays for photonuclear physics.
- *Spatial resolution from micrometers to nanometers*: Enriched beam-size options, such as sub-micrometer X-ray beams for membrane protein structure analysis; spatial resolution of tens of nanometers by X-ray nanoprobe or X-ray nano-CT for analysis of elemental mapping, chemical state, and nanostructures in environmental science, material science, and industry applications. Striking examples are lithium-ion batteries or nanoscale semiconductor devices.
- *Time resolution from milliseconds, microseconds to picoseconds*: Many enriched time resolution options for observing electron/atomic/molecular structures on picosecond, nanosecond, microsecond, or millisecond time scales in the rapid reaction process of a catalytic system to recognize the catalytic active site and selectivity, clarify the catalytic reaction process, and reveal the catalytic mechanism; to observe the microstructural evolution of polymer materials on a millisecond time scale during the impact process; and to investigate the deformation and failure behavior of materials under impact loading and high-speed fuel spray processes of automotive engines by picosecond X-ray single pulse imaging.
- *Industry applications*: Long beamlines for in situ monitoring of the structural evolution process of polymers in

✉ Ren-Zhong Tai
tairz@sari.ac.cn

Zhen-Tang Zhao
zhaozt@sari.ac.cn

[1] Shanghai Advanced Research Institute, Chinese Academy of Sciences, Shanghai 201204, China

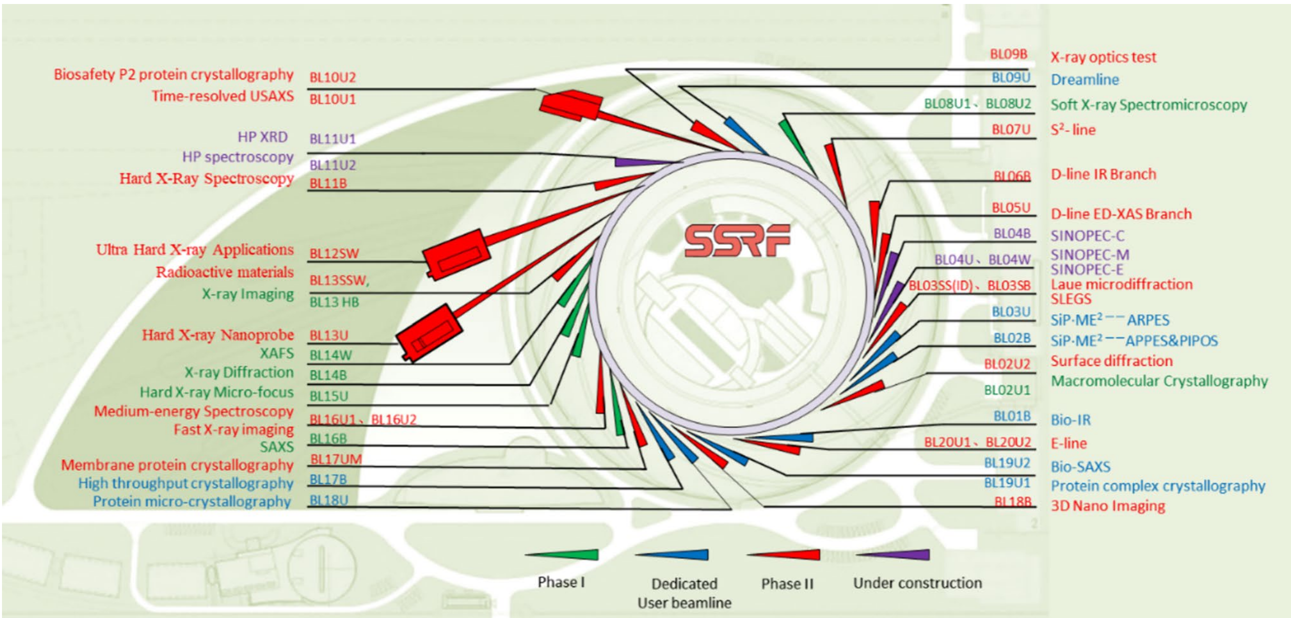

Fig. 1 **(Color online)** Layout of SSRF Beamlines. Phase-I beamlines, dedicated user beamlines, Phase-II beamlines, and beamlines under construction are distinguished by different colors

pilot-scale experiments and in situ characterization of engineering materials of large sizes in a serving environment.

- *High sensitivity*: Chemical sensitivity (1 ppb) and single-atom-level detection capability for environmental and geological sciences.
- *Techniques combining multiple regions of the spectrum*: To observe the same dynamic process from different viewpoints by combining complementary synchrotron radiation techniques, for example, the combination of X-rays and infrared (IR) can simultaneously detect the atomic, electronic, and molecular structures, and the combination of hard and soft X-rays can detect the electronic and chemical structures of a film layer by layer.
- *Hazardous and radioactive samples*: Biosafety P2 protection facilities dedicated to the macromolecular crystal structure analysis of moderate-risk infectious viruses; radioactive protection facilities dedicated to the composition and structure characterization of radioactive materials.
- *User data center*: For mass user data storage, real-time data analysis, deep data mining, artificial intelligence, and automation.

2 Accelerator upgrades

To meet the requirements of these new beamlines in the project, the storage ring has been upgraded accordingly, including the replacement of dipoles with super-bends in two cells, the construction of a 650-W helium cryogenic system, the development of a bunch-length control system, and an upgrade of the beam diagnostics and control systems.

The SSRF lattice was modified with two super-bend-based DBA cells, and two straight sections (ID11, ID16) were inserted in a quadrupole triplet so that each creates double mini-β_y optics for accommodating dual canted undulators.

A 3rd harmonic superconducting cavity system was developed and installed to lengthen the bunch in the passive operation mode. A 650-W helium cryogenic system was built to support the 3rd harmonic superconducting cavity and the superconducting wiggler, which can be switched to support the main RF cavities as backup when the phase-I cryogenic system fails. The hybrid filling pattern of the storage ring allows a single bunch current of up to 24.5 mA and a bunch train of 200 mA in the ring with the help of a transverse feedback system and a 3rd harmonic cavity, which can suppress instabilities and stretch the bunch length. This hybrid filling mode provides powerful support for single-pulse imaging and pump-probe transient structure research. The main parameters of the storage ring are listed in Table 1.

3 New beamlines

Sixteen beamlines (including one RIXS station) were built in this project, the main specifications of which are listed in Table 2. The photon energy extends to previously uncovered regions, such as the tender X-ray region,

Table 1 Main parameters of the storage ring

Parameters	Before phase-II	After phase-II
Beam energy (GeV)	3.5	3.5
Circumference (m)	432	432
Emittance (nm·rad)	3.89	4.22 (with superconducting wiggler)
Energy spread	9.8×10^{-4}	11.1×10^{-4}
Straight section (numbers × length (m))	4 × 12, 16 × 6.5	4 × 12, 16 × 6.5, 2 × 1.9
Beam length (mm)	3.8	4 – 8
Beam current, multi-bunch/single-bunch (mA)	200 – 300/5	200 – 300/20
Critical energy of normal/super-bend magnet radiation (keV)	10.3/–	10.3/18.7

super-hard X-ray region, and low-energy gamma-ray region. Beamline design has strengthened support for the industry. In practice, the design and construction of beamlines are extremely difficult. For example, one straight section usually has to consider supporting two beamlines to allow as many beamlines as possible for use, one beamline usually connects multiple end-stations to provide more methodology choices for users, and several experimental end-stations will realize state-of-the-art techniques that combine multiple regions of the spectrum with challenging technical difficulties that need to be solved.

In this paper, a brief description of the new beamlines is introduced, and a detailed description of this special issue can be found.

4 User experimental support

The experimental support for users includes materials laboratories, chemical laboratories, biomedical laboratories, in situ instrumentation pools, and user data centers. They are another essential part of the SSRF Phase-II beamline project with the goals of serving users in various aspects and effectively improving the comprehensive experimental capabilities at the SSRF.

(1) The material preparation laboratory satisfies the user requirements for material sample preparation. It provides sample preparation and auxiliary measurements for high-pressure materials, micro- and nanomaterials, etc.

- *Powder sample pressing*: 5–8 mm
- *High-temperature treating*: 25–1900 K
- *Thin film cutting*: 0.1–25 mm
- *SEM/TEM*: 3 nm/0.1 nm

(2) Chemical and environmental laboratory: Chemical sample preparation and on-site treatment, such as auxiliary component testing and auxiliary structure analysis

- *Operating environment*: $H_2O < 1$ ppm, $O_2 < 1$ ppm
- *Sample storage*: − 85 °C−10 °C
- *Particle crushing*: 40–150 μm

(3) Biology and medicine laboratory provides the basic experimental conditions for biomedical sample preparation on site, auxiliary testing of biomacromolecules and sample preparation, tissue sample preparation, and treatment.

- *Slice thickness*: 1–100 μm
- *Slice temperature*: − 35–0 °C, 5 K
- *Freezing rate*: 18,000 °C/s

(4) *In situ instrumentation pool*: This provides in situ equipment for the experimental station, such as for changing the temperature, pressure, vacuum, and magnetic field.

- *Temperature*: 4.5–2600 K
- *Magnetic field*: 0 – 8000 Gs
- *Vacuum transmission device*: 1.0×10^{-9} Torr
- *Tensile loading*: 5 kN

(5) *User data center*: With 23 PB storage, 11,000 CPU cores, 28 GPUs, and 19 edge clusters for beamlines, it provides mass data storage, real-time data analysis, deep data mining, and artificial intelligence and auto-

Table 2 The main specifications of SSRF phase-II beamlines

Beamlines	Source	Specifications	Scientific goals	Methods
E-line: hard X-ray soft X-ray	IVU EPU	Soft X-ray station: Energy range: 118–1560 eV. Energy resolution: 1.3×10^{-4} @ 244 eV. Beam size: 23.0 μm × 7.9 μm. Flux: 3.0×10^{12} phs/s@244 eV@0.1%BW	Energy conversion and control, Electron–hole excitation/charge order, Solid/liquid, interface	Resonant inelastic X-ray scattering (RIXS), Resonant X-ray elastic scattering (RXES)
		Hard X-ray station: Energy range: 2800–19,000 eV. Energy resolution: 1.9×10^{-4}@ 5000 eV. Beam size: 63.1.0 μm × 17.7 μm. Flux: 2.1×10^{12} phs/s @5000 eV@0.1%BW	Chemical and electronic structure in situ	X-ray emission spectroscopy (XES), High-energy resolution fluorescence detection (HERFD), X-ray Raman spectroscopy (XRS)
		The combined station: Energy range: 128.7–11,900 eV. Energy resolution: 1.8×10^{-4}@ 244 eV; 1.9×10^{-4}@ 5000 eV. Beam size: 92.7 μm × 42.2 μm@244 eV, 56.6 μm × 39.3 μm@5000 eV. Flux: 3.3×10^{12} phs/s@300 mA@244 eV@0.1%BW, 3.0×10^{12} phs/s @5000 eV@0.1%BW	Solid/gas, solid/solution interface, Layer-by-layer profile detection, Electronic structures, microscopy	Ambient-pressure X-ray photoelectron Spectroscopy (APXPS), Hard X-ray photoelectron spectroscopy (HAXPES), X-ray fine structure spectroscopy(XAFS)
D-Line: X-ray IR	IVU BM	Energy-dispersive XAS station: Energy range: 4.96 – 25.5 keV. Energy resolution: 2×10^{-4}@ Cu K-edge. Beam size (FWHM): 3.6 μm × 21.6 μm. Flux: 2.5×10^{12} phs/s·300 eV BW@7.2 keV. Time resolution: ~25 μs	Chemistry/catalysis, Condensed matter physics, Ultrafast transient structure	Time-resolved Energy-Dispersive XAS (ED-XAS), Extreme conditions, Pump-probe ED-XAS
		IR station: Spectral range: 10–10000 cm^{-1}. Spectral resolution: 0.1 cm^{-1}. Flux: 3.2×10^{13}phs/s/0.1% BW@ 4200 cm^{-1} @300 mA. Beam size: 23 μm × 24 μm@1000 cm^{-1}(Full width, Diffraction limit)	Chemistry, materials, biology, medicine	IR spectroscopy; IR microspectroscopy; Nano-IR spectroscopy
		The combined station: Energy range: 5–25 keV; Spectral range: 50–10000 cm^{-1}. Energy resolution: 2×10^{-4}@ CuK K-edge; Spectral resolution: 13.1 cm^{-1}(FTIR rapid scan) Beam size (FWHM):3.6 μm × 21.6 μm, 15.1 μm (H) × 25.8 μm (V)@1000 cm^{-1}. Flux: 2.5×10^{12} phs/s@300 eV BW@7.2 keV; 2.8×10^{13} phs/s/0.1%b.w. @4200 cm^{-1} @300 mA. Time resolution: 8.7 ms (FTIR); ~ 25 μs (ED-XAS)	Time-resolved atomic, electronic, and molecular structures in non-equilibrium systems	Energy-Dispersive XAS + IR microspectroscopy. Energy-Dispersive XAS + DRIFTS

Table 2 (continued)

Beamlines	Source	Specifications	Scientific goals	Methods
Radioactive materials	W	Beamline: Energy range: 4.97–50.24 keV. Energy resolution: 2.2×10^{-4} @20 keV. Beam size: 384 μm × 315 μm; 10.5 μm × 14.4 μm. Flux: 3.3×10^{12} phs/s@300 mA; 5.8×10^{10} phs/s@300 mA, microfocus. End-station: Sample radioactive activity: ≤ 1.85 GBq/Sample (α/β emitter); ≤ 185 MBq/Sample (γ emitte). HRXRD angle resolution: 0.009°@20 keV, HRXES energy resolution: 2.8 eV@13.618 keV	Detection of radioactive materials of sample activity up to 185 MBq/sample (γ emitter) and 1.85 GBq/sample (α/β emitter), Physics and chemistry related to radioactive materials. Nuclear fuels and waste, radioactive contaminations, radiation chemistry	XAFS, XES, XRD, XRF, and Imaging
Hard X-ray spectroscopy	BM	Energy range: 4.9–31.6 keV. Energy resolution: 1.31×10^{-4} @10 keV. Beam size: 214 μm × 244 μm. Flux: 4.98×10^{11} phs/s @10 keV	Catalysis	X-ray absorption fine structure (XAFS). Quick-scanning XAFS. Combined XAFS and XRD. In situ XAFS
Hard X-ray nanoprobe	IVU	High flux mode: Energy range: 10 keV. Energy resolution: 0.76×10^{-2}@ 10 keV. Beam size: 27.53 nm × 23.31 nm@10 keV. Flux: 5.2×10^{9} phs/s @10 keV. High-energy resolution mode: Energy range: 4.95–25.65 keV. Energy resolution: 2×10^{-4}@10 keV. Beam size: 50 nm × 50 nm@10 keV. Flux:1×10^{9} phs/s @10 keV	Nanotechnology, material science, life science, environment science., components	X-ray fluorescence, X-ray nanodiffraction, X-ray near edge absorption spectroscopy, and coherent diffraction imaging
Medium-energy spectroscopy	IVU	Energy range: 2.08–16.20 keV. Energy resolution: 1.76×10^{-4}@ 2.5 keV. Beam size: 3.1 μm × 1.1 μm @10 keV(K-B), 0.32 μm × 0.23 μm@2.5 keV(sK-B). Flux: 3.74×10^{12} phs/s @2.5 keV(K-B), 3.69×10^{12} phs/s @10 keV(K-B). Detection Limit: 4.1 ppb@Cu K-edge	Environmental pollutants, Environmental Catalysis, Energy material, Biological element analysis	XAFS, XRF, TEY μXAFS μXRF TXRF
3D nanoimaging	BM	Energy range:4.97–14.35 keV. Energy resolution ($\Delta E/E$): 1.83×10^{-4}. Flux:1.84×10^{10} phs/s@8 keV@300 mA. Spatial resolution: 19.9 nm@TXM@8 keV	Nanoimaging	TXM Nano-CT Nanospectral imaging
S2-Line: Spatial and spin resolution ARPES and magnetism	Twin EPU	Energy range: 48.2–2007 eV. Energy resolution: 11,500@867 eV; 16,308@91 eV; Beam size: 69.3 μm × 48.3 μm@Spin-ARPES; 200 nm × 200 nm@Nano-ARPES; Flux: 2.89×10^{11} phs/s/0.01%BW@867 eV, 300 mA, 9.48×10^{9} phs/s/0.01%BW@91 eV, 300 mA	Magnetic and electronic properties	Nano-ARPES; Spin-ARPES; XMCD/XMLD

Table 2 (continued)

Beamlines	Source	Specifications	Scientific goals	Methods
RIXS station	EPU	RIXS station: Energy range: 244.5–1845 eV. Energy resolution: 59.3 meV@930 eV. Beam size: 40 μm × 10 μm ($H \times V$). Flux: ≥ 1.52×10^{10} phs/s/0.01%BW@930 eV@ 300 mA. Sample temperature: 10.7 ~300 K	Collective excitations in quantum materials. Charge transfer in Energy materials	Resonant Inelastic X-ray Scattering X-ray emission spectroscopy
Laue microdiffraction	Super B	Materiel station: Energy range: 7–30 keV (white beam). Energy resolution: 0.96×10^{-4}@10 keV. Beam size: 0.9 μm × 1.3 μm. Flux: 4×10^{13} phs/s@300 mA (white beam). Protein Station: Energy range: 7–20 keV (white beam). Energy resolution: 0.96×10^{-4}@10 keV. Beam size: 4.2 μm × 4.3 μm. Flux: 6×10^{14} phs/s@300 mA (white beam)	Local microstructure and defects Laue Crystallography	Laue diffraction Fluorescence Serial protein X-ray crystallography, in-site data collection
Surface diffraction	CPMU	Energy range: 4.7–28 keV. Energy resolution: 1.3×10^{-4} @10 keV. Flux: 6.3×10^{12} phs/s@10 keV. Beam divergence: 42 μrad × 17 μrad. Beam size: 102 μm × 73 μm	Surface and interface of low-dimensional thin films Solid–liquid, liquid–liquid interfaces. Biomembrane structure, self-assembly in soft matte	Grazing Incident X-ray Diffraction X-ray Reflectivity Crystal truncation rods. Liquid X-ray scattering
Shanghai laser electron gamma source	ID	Energy range: 0.25–21.7 MeV. Flux: 2.14×10^{4} phs/s@20°–7.99×10^{6} phs/s@180°. Energy resolution 4.26% @180° with collimator. Angle divergence: 0.38 mrad	Nuclear Physics/Nuclear astrophysics/Gamma Source Application	Photonuclear Reaction
P2 protein crystallography	IVU	Energy range: 6.5–18.1 keV. Energy resolution: 1.78×10^{-4}. Beam size: 16.8 μm × 9.4 μm. Flux: 2.52×10^{12} phs/s (@12.7 keV, 300 mA) Biosafety: Level-2. Sample changer: Swordfish	Moderate-risk infectious viruses	Shutterless data collection, MR, MAD/SAD, In situ Data collection
Membrane protein crystallography	CPMU	Energy Range: 4.97–25.51 keV; Energy resolution: 1.75×10^{-4}@ 12 keV & DCM, Flux: 3.07×10^{11} phs/s (DCM@300 mA@12 keV @ 0.75 μm × 0.65 μm); 3.23×10^{12} phs/s (DMM@300 mA@12 keV @0.70 μm × 0.68 μm). Beam size: 0.7–20 μm. Data collection time: 32 s (360°). Sample measuring speed: 49 crystals/h	Membrane protein	Macromolecular crystallography; Micro-protein crystallography (μ-MX); Quasi-serial protein x-ray crystallography (SF); The multi- and single-wavelength anomalous dispersion (MAD/SAD)
Ultra-hard X-ray applications	SCW	Energy range: 29.7–162 keV. Beam size: 300 μm–100 mm. Energy resolution: 5×10^{-3}. Flux: 2.3×10^{11}phs/s@100 keV@25 μrad	Engineering materials and geological science	High-energy EDXRD, XRD, Imaging, PDF

Table 2 (continued)

Beamlines	Source	Specifications	Scientific goals	Methods
Time-resolved USAXS	IVU	Beamline: Energy range: 8~15 keV. Energy resolution: 5.8×10^{-3}@10 keV. Flux: 1.1×10^{13} phs/s@10 keV @300 mA. Beam size: 379 μm × 341 μm @10 keV ($H\times V$)		
		USAXS end-station: Time resolution: ~ 1.3 ms. $q_{\min}=0.0030$ nm^{-1}	In situ monitoring of structural evolution process in polymer processing and fiber-spinning at nm – μm scale	Time-resolved USAXS
		Micro-SAXS end-station: Flux: 3.2×10^{12} phs/s@10 keV @300 mA. Beam size: 7.6 μm × 4.3 μm @10 keV($H\times V$). $q_{\min}=0.049$ nm^{-1}	Local microstructure study by microfocus X-ray scattering	Microfocus SAXS/WAXS
		Industrial application end-station. Flux: 1.1×10^{13} phs/s@10 keV @300 mA. Tensile range of in situ stretching device: 0–4300 N. Temperature range of in situ stretching device: RT-520 °C	Industrial application	Time-resolved SAXS/WAXS
Fast X-ray imaging	CPMU	Energy range: 8.3– 30.5 keV. Energy resolution: 1.6×10^{-4}@ 10 keV. Beam size: 2.64 mm × 1.87 mm. Flux: 2.39×10^{13} phs/s @10 keV;1.31×10^{16} phs/s (white beam); 1.5×10^{9} phs (single pulse). Spatial resolution: 0.7 μm. Temporal resolution of single-pulse ultrafast X-ray imaging: 60 ps; Temporal resolution of X-ray dynamic imaging: 2 μs; Temporal resolution of X-ray dynamic micro-CT: 50 ms	Fast process imaging	Single-pulse ultrafast X-ray imaging. Microsecond-resolved X-ray dynamic imaging. Millisecond-resolved X-ray dynamic micro-CT. High-resolution quantitative micro-CT

mation. A schematic view of the big data framework in the user datacenter is shown in Fig. 2.

- *CPU + GPU*: Rpeak 967 Tflops
- *Store capacity*: 23 PB HDD + 100 TB SSD
- *Bandwidth to beamline*: 40 GB/s

5 Beamline technique support

The beamline technique support supports the construction of optics, mechanical engineering, control and electronics, engineering analysis, and test beamlines. The primary specifications of the X-ray test beamline are listed in Table 3. As an essential part of the SSRF Phase-II Beamline Project, beamline technique support will provide solutions for various key technical issues regarding the development, installation, tuning, and testing of the equipment used at beamlines. In the future, they will ensure the highly efficient operation of the beamlines.

High-performance X-ray optics are the basis and prerequisites for the construction of advanced synchrotron radiation beamlines and experimental stations. Highly brilliant and coherent X-rays are deflected, collimated, changed to be monochromatic, and focused by a series of optical components before being delivered to the sample for scientific experimental research. Therefore, the full utilization of the coherent wavefront and ultrahigh brightness of advanced X-ray light sources depends on the performance of the optical components. Through domestic cooperation and taking advantage of the high-precision optical metrology technology developed by the SSRF, a 1000-mm-long plane mirror with a 0.2-μrad slope error and a multilayer monochromator have been successfully developed.

High-performance key equipment guarantees the construction of advanced beamlines for the project. A series of core equipment was developed to meet the requirements of the beamlines in the SSRF Phase-II beamline project. For example, the high-energy sagittal-focusing Laue monochromator can achieve small radius dynamic bending of ultra-thin crystals, and the size of the focusing spot reached 260 μm. The cryo-cooled meridian bent Laue monochromator was first domestically developed and has passed the test acceptance. The plane-grating monochromator realized cryo-cooling of high heat load plane mirrors for the first time. Meanwhile, a number of general key equipment, such as a sub-microradian mirror bender system, a cryo-cooled double crystal monochromator, and a precision monochromatic slit have also been developed. The slope error of the mirror bender was less than 0.4 μrad (RMS), and the bending curve resolution and repeatability of the bender were less than 0.5% ($\Delta R/R$). The relative stabilities of the first and second DCM crystals were 63 nrad (RMS). The performance of this general key equipment meets the requirements of most beamlines in the project.

The control systems were designed using the EPICS (Experimental Physics and Industrial Control System) [5] and the Bluesky Data Collection Framework. The system supports motion control, detector control, and equipment protection at the beamlines. Hardware for stepper motor control was developed. The synchronization accuracy of the hardware for fly scanning reaches 20 ns, which can meet most requirements for fly scanning experiments. A beam position monitor (BPM) and its current front-end amplifier have been developed successfully with precisions of 1 mm and 1 pA, which can play important roles in nanometer positioning feedback control. The control system is

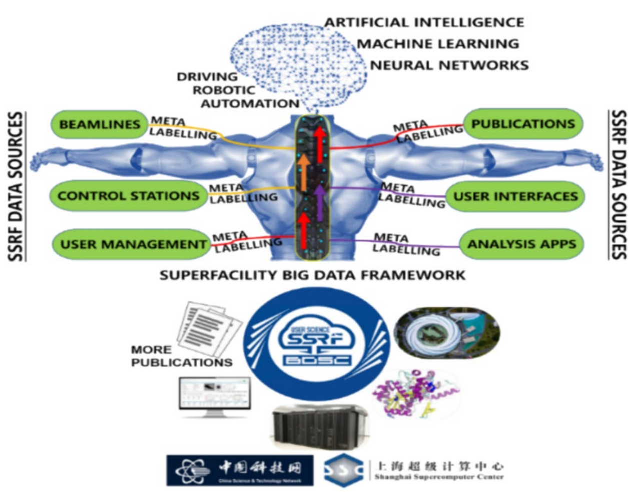

Fig. 2 **(Color online)** A schematic view of the big data framework in the user data centre, encompassing experiments, scientific computing, data acquisition, storage, analysis, management and visualization, aimed at increasing the SSRF users' scientific productivity, leveraging big data, AI, robotic automation, HPC, and national supercomputing technologies

Table 3 The main specifications of the X-ray test beamline

Beamlines	Source	Specifications	Scientific goals	Methods
X-ray test beamline	BM	Energy range: 4–30 keV. Energy resolution: 5×10^{-4} @10 keV. Beam size: 500 μm × 400 μm@10 keV. Flux: 3×10^{11} phs/s @10 keV	High-performance beamline instrument and optics	XRD/XRF/XAFS Imaging

Fig. 3 **(Color online)** Bird view of SSRF

equipped with single-pulse timing synchronization control and measurement instruments, such as an event timing system and a streak camera, which can support the timing control of picosecond time-resolved pump-probe experiments. EPICSv7, the most cutting-edge EPICS technology, has been researched and used in a control laboratory to overcome the bottlenecks of big data communication and enhance the overall performance of the control system.

6 Conclusion and perspectives

Since its first operation in 2009, the SSRF has greatly accelerated the development of photon science in mainland China. The completion of the SSRF Phase-II beamline project is believed to bring the experimental capability of the SSRF to a new level, with rich and diverse choices in photon energies, methodologies, and in situ conditions, mutual promotion of offline and online experiments, rapid data processing and analysis, and various resolution abilities close to the limit of the third-generation light source. Figure 3 shows the latest bird's-eye view of the SSRF.

The construction of the SSRF Phase-II project has been conducted, while the SSRF is still in operation, which brought great challenges to project management, installation, and testing. The first beamline, the hard X-ray spectroscopy beamline, was completed and began commissioning at the end of 2018, whereas the last two beamlines, the hard X-ray nanoprobe beamline and the medium-energy spectroscopy beamline, were completed at the end of July of that year. Till the end of 2023, SSRF Phase-II beamlines have provided 45,741 h of beam time and executed a total of 1152 research proposals from 678 research teams, with 368 user papers published, including seven CNS papers [6–12]. The next step is to optimize machine performance for stable operation and to organize and promote large scientific research projects.

To date, 34 beamlines in the SSRF are in operation, and nearly 100 types of advanced experimental methods have been realized. This systematic and state-of-the-art experimental facility for third-generation synchrotron radiation, particularly the SSRF Phase-II beamline project, is anticipated to contribute significantly to cutting-edge science and technology.

References

1. M. Jiang, X. Yang, H. Xu et al., Shanghai synchrotron radiation facility. Chin. Sci. Bull. **54**, 4171–4181 (2009). https://doi.org/10.1007/s11434-009-0689-y
2. Shanghai Synchrotron Radiation Facility (SSRF), https://www.nst.sinap.ac.cn/newAlbumDetail/112/218/en/, 2023, [accessed 5 November 2023]
3. SSRF Phase-II Beamlines, https://link.springer.com/collections/cibbjfaddc 2023, [accessed 5 November 2023]
4. R. Tai, Z. Zhao, Commissioning and first results of the SSRF Phase-II beamline project. J. Phys. Conf. Ser. **2380**, 012004 (2022). https://doi.org/10.1088/1742-6596/2380/1/012004
5. L. Shen and D. Liu, Present status of SSRF control system. in *Proceedings of ICALEPCS07*, Knoxville, Tennessee, USA, 15–19, October (2007)
6. G. Cao, J. Liang, Z. Guo et al., Liquid metal for high-entropy alloy nanoparticles synthesis. Nature **619**, 73–77 (2023). https://doi.org/10.1038/s41586-023-06082-9
7. L. Li, H. Liao, Y. Meng et al., Structural basis of human ACE2 higher binding affinity to currently circulating omicron SARS-CoV-2 sub-variants BA.2 and BA.1.1. Cell **185**(16), 2952–2960.e10 (2022). https://doi.org/10.1016/j.cell.2022.06.023
8. P. Han, L. Li, S. Liu et al., Receptor binding and complex structures of human ACE2 to spike RBD from omicron and delta SARS-CoV-2. Cell **185**, 630-640.e10 (2022). https://doi.org/10.1016/j.cell.2022.01.001
9. Z. Liang, Y. Zhang, H. Xu et al., Out-of-plane cations homogenise perovskite composition for solar cells. Nature **624**, 557–563 (2023). https://doi.org/10.1038/s41586-023-06784-0
10. J. Jeong, M. Kim, J. Seo et al., Pseudo-halide anion engineering for α-FAPbI3 perovskite solar cells. Nature **592**, 381–385 (2021). https://doi.org/10.1038/s41586-021-03406-5

11. Y. Shang, Z. Liu, J. Dong et al., Ultrahard bulk amorphous carbon from collapsed fullerene. Nature **599**, 599–604 (2021). https://doi.org/10.1038/s41586-021-03882-9
12. S. Feng, M. Bai, I. Rivas-González et al., Incomplete lineage sorting and phenotypic evolution in marsupials. Cell **185**, 1646-1660.e18 (2022). https://doi.org/10.1016/j.cell.2022.03.034